



HHS Public Access

Author manuscript

Org Biomol Chem. Author manuscript; available in PMC 2015 August 07.

Published in final edited form as:

Org Biomol Chem. 2014 August 7; 12(29): 5375–5381. doi:10.1039/c4ob00886c.

Comparison of Backbone Modification in Protein β -Sheets by $\alpha \rightarrow \gamma$ Residue Replacement and α -Residue Methylation

George A. Lengyel, Zachary E. Reinert, Brian D. Griffith, and W. Seth Horne

Department of Chemistry, University of Pittsburgh, Pittsburgh, PA 15260, USA

W. Seth Horne: horne@pitt.edu

Abstract

The mimicry of protein tertiary structure by oligomers with unnatural backbones is a significant contemporary research challenge. Among common elements of secondary structure found in natural proteins, sheets have proven the most difficult to address. Here, we report the systematic comparison of different strategies for peptide backbone modification in β -sheets with the goal of identifying the best method for replacing a multi-stranded sheet in a protein tertiary fold. The most effective sheet modifications examined lead to native-like tertiary folding behavior with thermodynamic fold stability comparable to the prototype protein on which the modified backbones are based.

Introduction

Synthetic oligomers with the capacity to adopt discrete folded structures (“foldamers”)¹ have received significant research attention,² due in part to their ability to mimic natural peptide folding patterns. In more than two decades of work showing increasingly sophisticated structures from unnatural backbones, tertiary folds like those commonly found in proteins have proven difficult to recreate. Although significant progress has been made with helix-turn-helix targets,³ these represent only a small fraction of the diverse array of folds found in nature. Reproducing a wider selection of natural protein structural motifs with unnatural oligomers is an important goal because it opens the door to reproducing the full repertoire of functions enabled by those folds.

One design concept that shows promise in addressing the challenge of tertiary structure mimicry is the systematic backbone alteration of natural sequences. Folded proteins can tolerate diverse backbone modifications without compromising sequence-encoded folding.⁴ Bridging the gap between these observations and precedent on *de novo* foldamer design² suggests an approach toward protein mimicry, in which a number of α -residues in a sequence with known folding behavior are replaced with various unnatural building blocks to generate heterogeneous backbones capable of adopting native-like folds. The versatility of the above method for mimicry of isolated α -helix⁵ and β -sheet⁶ secondary structures has

Correspondence to: W. Seth Horne, horne@pitt.edu.

†Electronic Supplementary Information (ESI) available: Figures S1–S3, Tables S1–S8, and experimental methods for the synthesis of unnatural amino acid monomers. See DOI: 10.1039/b000000x/

recently been leveraged to simultaneously modify all the secondary structures in a small protein tertiary fold.⁷ A fundamental question that must be addressed for sequence-guided backbone alteration to be effective for the widest array of target folds is how to best apply chemical modification without disrupting sequence-encoded folding.

Among common protein secondary structures, sheet folds have proved more challenging targets than helices or turns for mimicry by unnatural oligomers. Building on pioneering work carried out largely in organic solvents,⁸ we have recently focused on developing strategies for the design of heterogeneous-backbone β -sheet mimics that fold in water.⁶ Hairpin model systems, widely used in fundamental studies on β -sheet formation in proteins,⁹ have proved valuable in assessing sheet propensity of unnatural building blocks. Unfortunately, the lessons learned in the hairpin context are not always applicable in a more complex protein tertiary fold. As an example, when incorporated in each strand of a hairpin-forming peptide, appropriately substituted β -amino acid residues (homologated analogues of α -residues) can maintain native-like folding,^{6a,6b} but the same modifications abolish folding entirely when made in a four-stranded β -sheet in a small protein.⁷

Here, we report the side-by-side comparison of several different strategies for peptide backbone modification in β -sheet secondary structures with the goal of identifying the best method for replacing a multi-stranded sheet in a protein tertiary fold. The most effective sheet modifications examined lead to native-like tertiary folding behavior with thermodynamic fold stability comparable to the prototype protein on which the modified backbones are based.

Results and Discussion

Strategies Examined for Sheet Backbone Alteration

We compared three strategies for peptide backbone alteration in two different β -sheet forming host sequences – a two-stranded hairpin peptide and a four-stranded sheet in a small protein tertiary fold (Figure 1). α -Residues in each prototype sequence were replaced with *N*-methylated analogues ($\alpha \rightarrow N\text{-Me-}\alpha$), (*E*)-vinyllogous γ^4 -residues ($\alpha \rightarrow \gamma^4$), or the cyclically constrained γ -residue Acc ($\alpha \rightarrow \gamma^{\text{cyc}}$). These three backbone modifications and some of the unanswered questions we sought to address about each are discussed in more detail below.

Methylation of backbone amide nitrogen atoms has been widely applied in small peptides¹⁰ and can be used to modify capping strands of sheet-forming sequences.¹¹ We recently showed $\alpha \rightarrow N\text{-Me-}\alpha$ residue substitution is accommodated in a small bacterial protein, but it resulted in a degree of destabilization that was surprising given the subtle nature of the chemical change.⁷ One goal in the present work was to elucidate the molecular basis of this destabilization by systematically examining the site-dependent structural and thermodynamic effects of *N*-methylation on the folding of a small hairpin sequence.

In another effort toward sheet mimetics based on systematic modification of natural sequences, we recently reported that the cyclically constrained γ -residue (1*R*,3*S*)-3-aminocyclohexane carboxylic acid (Acc) can be incorporated into a hairpin-forming α -peptide sequence ($\alpha \rightarrow \gamma^{\text{cyc}}$ substitution in each strand) without significantly altering the

folded structure.^{6c} Interestingly, the fold of the chimeric $\alpha/\gamma^{\text{cyc}}$ -peptide was actually more thermodynamically stable than that of the prototype α -peptide on which it was based.^{6c} A second open question we wanted to address in this study is whether such $\alpha \rightarrow \gamma^{\text{cyc}}$ substitutions are tolerated in the complex structural environment of a multi-stranded sheet in a protein tertiary fold.

A third strategy examined for backbone modification in β -sheets involved the replacement of α -residues with γ -residues bearing a side chain at C_γ and an (*E*)-double bond between C_α and C_β . These vinylogous γ^4 -residue building blocks are known to be compatible with hairpin formation in organic solvent,^{8a,8f} but their impact on folding in aqueous environments has not been reported. γ^4 -Residues offer an advantage over the γ^{cyc} residue Acc in that they can retain protein-derived side chains when they replace α -residues in a native sequence. We incorporated vinylogous γ^4 -residues ($\alpha \rightarrow \gamma^4$ substitution in each strand) into both peptide hairpin and protein sheet contexts in order to ascertain the compatibility of these residues with the native folds.

Backbone Alteration in a Peptide β -Hairpin Host Sequence

Peptide hairpin **1** (Figure 2), derived from the C-terminal segment of the B1 domain of Streptococcal protein G,¹² has proven a useful host sequence for exploring the sheet folding propensities of modified peptide backbones in aqueous solution.^{6b,6c} Sequences **2–7** are variants of peptide **1** designed to systematically compare the impact of the different strategies for backbone alteration described above on the structure and stability of the sequence-encoded hairpin fold.

In peptide **2**, α -residues Ala₄ and Ala₁₃ in **1** are replaced by the constrained γ^{cyc} -residue Acc ($\alpha \rightarrow \gamma^{\text{cyc}}$ substitution). We have previously reported the synthesis and biophysical analysis of **2**, and it is included here as a point of comparison.^{6c} Peptide **3** has the same sites of backbone modification as **2**, but the unnatural building blocks are vinylogous γ^4 -residues bearing the side chain of the replaced α -residues in **1** ($\alpha \rightarrow \gamma^4$ substitution). In peptides **4–7**, α -residues Trp₃, Tyr₅, Phe₁₁, or Val₁₃ from host sequence **1** are individually modified by *N*-methylation ($\alpha \rightarrow N\text{-Me-}\alpha$). These four sites, all at non-hydrogen-bonding positions in the hairpin, were modified separately to determine how sequence context influences the thermodynamic impact of *N*-methylation on hairpin folded stability.

Peptides **1–7** were synthesized by Fmoc solid-phase peptide methods, purified by reverse-phase HPLC, and the identities of the purified oligomers confirmed by mass spectrometry. We compared the folding behavior of **1–7** by a series of multidimensional NMR experiments carried out in pH 6.3 phosphate buffer at 5 °C. Homonuclear ¹H–¹H COSY, TOCSY, and NOESY spectra were sufficient to enable full resonance assignment of each oligomer. As described in prior work, we used the chemical shift separation of the two diastereotopic H_α's in Gly₁₀ to quantify folded population and estimate folding free energy in the modified hairpins (Table 1).^{6b,6c,12–13}

Comparison of the NMR data for peptides **2** and **3** suggests that the connectivity of the γ -residue incorporated into each strand of the hairpin has a significant effect on folding energetics. We previously showed that peptide **2**, which contains two $\alpha \rightarrow \gamma^{\text{cyc}}$ substitutions

relative to **1**, forms a more stable hairpin than the wild-type backbone.^{6c} In contrast, the $\alpha \rightarrow \gamma^4$ substitutions in peptide **3** measurably destabilized the fold (~ 0.6 kcal mol⁻¹ relative to prototype **1** and ~ 1.1 kcal mol⁻¹ relative to variant **2** with the Acc residues).

In considering the different impact of γ^{cyc} and γ^4 residues on hairpin folded stability, we saw two possible origins: a significant change in the folded structure or altered backbone flexibility. In order to test the former hypothesis, we pursued a solution structure of **3** by simulated annealing with NMR-derived distance restraints and compared the resulting coordinates to the previously determined structure of γ^{cyc} -residue-containing variant **2**. Due to the low folded population of **3**, we synthesized a cyclic derivative for NMR structural analysis (**3_{cyc}**), which has Cys residues appended to each terminus and linked together via a disulfide bond. α/γ^4 -Peptide **3_{cyc}** forms a β -hairpin fold very similar to that of α/γ^{cyc} -peptide **2** (Figure 3). The similarity among the solution structures of **2** and **3_{cyc}** suggest the different number of freely rotatable bonds in the two γ -residue classes (three for each unsaturated γ^4 vs. two for each γ^{cyc}) is likely responsible for the different folded stabilities of the hairpins containing them.

Analysis of the NMR data for peptides **4–7** reveals two important issues with respect to backbone *N*-methylation in sheet-forming sequences. First and most pronounced are complications arising from *cis/trans* amide isomerization.^{10,14} Each *N*-methyl hairpin showed signals for two distinct species by NMR, which we attributed to a mixture of *cis* and *trans* isomers at the tertiary amide introduced upon *N*-methylation. We calculated the isomer ratio by integrating well-resolved peaks in the TOCSY spectra. Population ratios varied among the four oligomers, but the *trans* amide was predominant in each case. We made this assignment based on analysis of the NOESY data, which showed close contacts between the backbone methyl group in the *trans* isomer and both the side-chain and H _{α} protons of the preceding residue. The consistently lower Gly H _{α} /H _{α'} chemical shift separation indicates the presence of a *cis* amide in the chain destabilizes the hairpin fold considerably. This is reasonable considering how such a change would disrupt backbone direction and side chain contacts that enable parent sequence **1** to fold.

Separate from the issue of amide isomerization in *N*-Me- α -peptides **4–7** is the question of how the folded stability of the all-*trans* isomers compare to α -peptide **1**. The answer depends on the positioning of the backbone methyl group relative to the hairpin turn. The presence of an *N*-methyl amide in a *trans* configuration at either Trp₃ (peptide **4**) or Val₁₄ (peptide **7**) led to a folded population identical within error to that of prototype sequence **1**. By contrast, when the site of backbone methylation was closer to the turn (peptides **5** and **6**), the folded state was measurably destabilized – even after taking into account the detrimental contribution of the *cis* isomer.

Computational studies have shown that the energetically accessible backbone conformations of *N*-Me- α -residues are more restricted than their non-methylated analogues.¹⁵ Notably, one region of the Ramachandran plot that becomes significantly disfavored energetically upon *N*-methylation corresponds to typical backbone dihedrals for strands from an antiparallel β -sheet.¹⁶ The above observations help to rationalize the observed destabilization of the hairpin folds of *trans*-amide isomers of *N*-Me- α -peptides **5** and **6** relative to α -peptide **1**.

Backbone Alteration in a Protein β -Sheet Host Sequence

As a host sequence to examine sheet backbone modification in the context of a tertiary structure, we employed the full-length 56-residue B1 domain of Streptococcal protein G (**8**, Figure 4). This sequence, from which hairpin peptide **1** is derived, adopts a compact tertiary fold consisting of an α -helix packed against a four-stranded β -sheet.¹⁷ Of the three backbone alteration strategies above, one has previously been examined in GB1: $\alpha \rightarrow N\text{-Me-}\alpha$ substitution at terminal strands in the sheet (protein **9**).⁷ We include data for protein **9** here for comparison. In proteins **10** and **11**, $\alpha \rightarrow \gamma$ residue substitutions are made in place of Ile₆, Glu₁₅, Thr₄₄, and Thr₅₃. Protein **10** incorporates constrained γ^{cyc} residues at these positions, while variant **11** bears vinylogous γ^4 -residues with side chains derived from the natural GB1 sequence. In both **10** and **11**, the positioning of γ -residues is designed to create a stripe of unnatural residues along the center of the sheet if the modified backbones adopt a native-like tertiary fold. Protein **12** is a variant of GB1 with a completely natural backbone but mutations that remove three polar side-chain functional groups that are lost upon incorporation of Acc residues in protein **11**. Finally, protein **13** is a variant of **11** with the same number of γ^{cyc} residues but incorporated at positions intended shift the stripe of unnatural monomers to a different region of the sheet.

We compared the folding behavior of proteins **8–13** by circular dichroism (CD) spectroscopy in pH 7 phosphate buffer. CD scans (Figure 5A) for three of the four modified backbones (proteins **9**, **11**, and **13**) showed shapes and magnitudes similar to wild-type GB1. These results suggest $\alpha \rightarrow N\text{-Me-}\alpha$ substitution and two different patterns of $\alpha \rightarrow \gamma^{\text{cyc}}$ substitution are well tolerated in the tertiary fold. Protein **10**, bearing four $\alpha \rightarrow \gamma^4$ residue replacements, had a CD spectrum qualitatively different from all the other GB1 analogues examined. Its dissimilarity to typical random coil signatures and dependence on temperature (*vide infra*) argue against **10** existing as an unstructured chain. We cannot definitively say whether the spectrum of **10** is a result of an altered folded state or a change in the CD signature of the native-like tertiary fold due to the presence of four α, β -unsaturated amides in the backbone. In an effort to clarify this point, we attempted to obtain diffraction-quality crystals of protein **10** but were unsuccessful.

We performed thermal denaturation experiments to determine the impact of backbone substitutions on folded stability, monitoring the CD minima at 220 nm as a function of temperature (Figure 5B). All the proteins showed sharp sigmoidal unfolding transitions with cooperativities similar to wild-type GB1. The steep thermal unfolding transitions suggest the modified oligomers have well-ordered folded states. Comparing the midpoints of the thermal unfolding transitions (T_m) provides an estimate of the energetic impact of various backbone alterations on folding (Table 2).

As reported previously, protein **9** bearing two $\alpha \rightarrow N\text{-Me-}\alpha$ substitutions has a stability only slightly lower than wild-type GB1.⁷ In contrast, $\alpha \rightarrow \gamma$ residue replacements in proteins **10** and **11** destabilize their folded states considerably. Consistent with their relative folding propensities in the hairpin host sequence, the γ^{cyc} Acc residues (protein **11**) are superior to vinylogous γ^4 residues (protein **10**) in supporting the tertiary structure when incorporated at identical positions in the host sequence.

In considering the data for α/γ -hybrid protein **11**, we found it striking that the γ^{cyc} residue Acc, which stabilized the hairpin secondary structure, was so destabilizing to the tertiary fold. One difference between protein **11** and wild-type **8** besides the altered backbone in the former is the loss of three functionalized side chains upon substitution of α -residues Glu₁₅, Thr₄₄, and Thr₅₃ with Acc. Inspection of the crystal structure of wild-type GB1 shows three of these side chains are involved in inter-strand polar contacts that potentially stabilize the tertiary fold. The CD thermal stability observed for protein **12**, which has a natural backbone but lacks polar groups necessary for these contacts, indicate that the lost side-chain functionality is at most a very small contributor to the difference in folding behavior between **11** and **8**.

Another factor we considered as potentially responsible for destabilization of the γ -residue modified proteins is the increase in backbone length by two atoms with each $\alpha \rightarrow \gamma$ residue substitution. When found in the core of the protein as in **10** and **11**, this change may disrupt critical hydrophobic contacts between the sheet and helix necessary for folding. In order to test this hypothesis, we examined an analogue of GB1 (protein **13**), bearing four Acc residues in a pattern that would create a stripe of γ -residues in the sheet as in **10** and **11** but further removed from the hydrophobic core of the protein in the folded state. We reasoned that the alteration in backbone length of the sheet would be better tolerated if it was not located in close proximity to key tertiary contacts. Supporting the above hypothesis, protein **13** showed a dramatically improved thermal stability compared to closely related analogue **11**.

Conclusions

In summary, we have reported here the systematic comparison of three different strategies for peptide backbone modification in β -sheet secondary structures using two different host systems – a hairpin peptide and a small protein with a defined tertiary fold. Our results provide new insights into the design of heterogeneous backbones based on natural peptide sequences that encode for β -sheet folds. In the peptide hairpin host sequence, $\alpha \rightarrow \gamma^{\text{cyc}}$ substitution was superior to $\alpha \rightarrow \gamma^4$, which was better than backbone methylation ($\alpha \rightarrow N\text{-Me-}\alpha$). Destabilization of the sheet fold by $\alpha \rightarrow N\text{-Me-}\alpha$ substitution appears to result primarily from population of an unproductive *cis* tertiary amide isomer at the methylation site, though the fold of the *trans* isomer is also destabilized relative to native due to local stereoelectronic effects. In the best case for hairpin modification ($\alpha \rightarrow \gamma^{\text{cyc}}$), the heterogeneous backbone had a more stable fold than the prototype α -peptide on which it was based.

When substitutions are applied to a central stripe of strand residues in the protein tertiary structure, the trend was significantly different than the hairpin host sequence: *N*-Me- α residue incorporation at capping strands of the sheet was best tolerated, followed by γ^{cyc} and vinylogous γ^4 substitutions in all four strands. Optimization of the placement of γ^{cyc} residues, however, had a dramatic effect on the thermodynamic consequences of the modification. Shifting the position of the backbone expansion resulting from $\alpha \rightarrow \gamma$ residue substitution away from the hydrophobic core of the protein led to a heterogeneous backbone with near wild-type folded stability. We anticipate these results will aid in ongoing efforts to

recreate β -sheet folding patterns from heterogeneous backbones and open the way toward design of protein-mimetic oligomers with increasingly diverse tertiary folding topologies.

Experimental

Peptide and Protein Synthesis

Protected γ^4 -amino acids were prepared via the corresponding α -amino aldehydes¹⁸ according to published methods.¹⁹ Fmoc-Acc was prepared as previously described.^{6c} Full experimental details and characterization data for new compounds are given in the Supporting Information (SI).

β -Hairpin peptides were synthesized using microwave-assisted Fmoc solid-phase synthesis techniques on a MARS microwave reactor (CEM) using NovaPEG Rink Amide resin. Couplings were carried out in NMP at 70 °C for 4 min using 4 equiv of Fmoc-protected amino acid, 4 equiv of HCTU, and 6 equiv DIEA. PyAOP was used in place of HCTU for the coupling of *N*-methylated residues and residues immediately following them. Deprotections were performed using an excess of 20% 4-methylpiperidine in DMF at 80 °C for 2 min. After each coupling or deprotection cycle, the resin was washed three times with DMF. Double couplings were performed at sequence positions following proline or *N*-methylated residues. Prior to cleavage, the resin was washed three times each with DMF, dichloromethane, and methanol, and then dried. Peptide cleavage was accomplished using 95% trifluoroacetic acid (TFA), 2.5% triisopropylsilane (TIS), and 2.5% water.

Peptide was precipitated from the cleavage solution by addition of diethyl ether and purified by preparative HPLC on a C18 column using gradients between 0.1% TFA in water and 0.1% TFA in acetonitrile. After purification, the linear precursor to peptide **3_{eye}** was dissolved in 10 mM pH 8.9 phosphate buffer with 5% v/v DMSO, stirred until analytical HPLC and MS showed complete conversion to the cyclic disulfide (**2 d**), and then purified by HPLC to obtain **3_{eye}**.

Protein GB1 and variants were synthesized on a PTI Tribute synthesizer using NovaPEG Rink Amide resin (70 μ mol scale). Coupling reactions were performed by combining 3 mL of 0.4 M *N*-methylmorpholine in DMF with 7 equiv Fmoc-amino acid and 7 equiv HCTU. Following a two minute preactivation, the activated amino acid was added to the resin and vortexed for 45 min. Deprotection reactions were carried out twice with 3 mL of a 20% v/v solution of 4-methylpiperidine in DMF for 4 min. The resin was washed three times with 3 mL of DMF for 40 s between each cycle. After the final deprotection step, the resin was washed with 3 mL of dichloromethane followed by 3 mL of methanol. Resin was dried and subjected to cleavage by treatment with a solution of 94% TFA, 1% TIS, 2.5% water, and 2.5% ethanedithiol. Crude protein was precipitated by addition of cold diethyl ether. The solid was pelleted by centrifugation and dissolved in 6 M guanidinium chloride, 25 mM sodium phosphate, pH 6. This solution was subjected to purification by preparative C18 reverse-phase HPLC using gradients between 0.1% TFA in water and 0.1% TFA in acetonitrile. Each protein was subjected to a second round of purification by anion-exchange chromatography on a monoQ 5/50GL column (GE Healthcare) using 0.02 M Tris buffer at pH 8 and eluting with increasing concentrations of KCl.

All peptides and proteins used for biophysical analysis were >95% pure as determined by analytical HPLC on a C18 column. Identities were confirmed by mass spectrometry using a Voyager DE Pro MALDI-TOF instrument (Table S1).

NMR Sample Preparation, Data Collection, and Analysis

NMR samples were prepared by dissolving peptide in 750–850 μL of degassed 50 mM phosphate, 9:1 $\text{H}_2\text{O}/\text{D}_2\text{O}$, pH 6.3 (uncorrected for the presence of D_2O) to a final concentration of 0.8–3 mM. 3-(Trimethylsilyl)-1-propanesulfonic acid sodium salt (DSS, 50 mM in water) was added to a final concentration of 0.2 mM. Each solution was passed through a 0.2 μm syringe filter, and transferred to an NMR tube. The NMR tube headspace was purged with a stream of nitrogen prior to capping.

NMR experiments were performed on a Bruker Avance-700 spectrometer. Chemical shifts are reported relative to DSS (0 ppm). TOCSY, NOESY, and COSY pulse programs used excitation-sculpted gradient-pulse solvent suppression. For all 2D experiments, 2048 data points were collected in the direct dimension and 512 data points in the indirect dimension. The mixing times for TOCSY and NOESY were 80 ms and 200 ms, respectively. NMR measurements were performed at a temperature of 278 K for hairpin peptides **3–7** and at 293 K for cyclized hairpin peptide **3_{cyc}**. The Sparky software package (T. D. Goddard and D. G. Kneller, SPARKY 3, University of California, San Francisco) was used to analyze 2D NMR data. Backbone chemical shift assignments for peptides **3–7** are reported in Tables S2–7. Analysis of NMR data for **3–7** and estimation of folded populations followed previously published methods.^{6b,6c} Tabulated NOEs for peptide **3_{cyc}** are reported in Table S8. These data were applied to calculate an NMR solution structure of **3_{cyc}** using the Crystallography and NMR system (CNS) software package²⁰ according to published methods.^{6b,6c}

Circular Dichroism Spectroscopy

CD measurements were performed on an Olis DSM17 Circular Dichroism Spectrometer in 2 mm quartz cells. Samples consisted of 40 μM protein in 20 mM sodium phosphate buffer, pH 7. Scans were carried out at 25 $^\circ\text{C}$ over the range of 200–260 nm in 1 nm increments with a 2 nm bandwidth. Scan data were smoothed by the Savitzky-Golay method. Melts were monitored at 220 nm over the range of 4 $^\circ\text{C}$ to 98 $^\circ\text{C}$ with 2 $^\circ\text{C}$ increments, a dead band of 0.5 $^\circ\text{C}$, and a 2 min equilibration time at each temperature. All measurements were baseline corrected for blank buffer. Temperature-dependent CD data were fit to a two-state unfolding model to obtain melting temperature (T_m). The change in free energy of folding for each mutant relative to wild-type (ΔG_{fold}) was estimated from the change in T_m (ΔT_m) using the enthalpy of folding determined for GB1 by differential scanning calorimetry.²¹

Supplementary Material

Refer to Web version on PubMed Central for supplementary material.

Acknowledgments

Funding for this work was provided by the University of Pittsburgh and the National Institutes of Health (R01GM107161).

Notes and References

1. Gellman SH. *Acc Chem Res.* 1998; 31:173–180.
2. (a) Bautista AD, Craig CJ, Harker EA, Schepartz A. *Curr Opin Chem Biol.* 2007; 11:685–692. [PubMed: 17988934] (b) Goodman CM, Choi S, Shandler S, DeGrado WF. *Nat Chem Biol.* 2007; 3:252–262. [PubMed: 17438550] (c) Horne WS. *Expert Opin Drug Discov.* 2011; 6:1247–1262. [PubMed: 22647064] (d) Guichard G, Huc I. *Chem Commun.* 2011; 47:5933–5941. (e) Pils LA, Reiser O. *Amino Acids.* 2011; 41:709–718. [PubMed: 21462000]
3. (a) Cheng RP, DeGrado WF. *J Am Chem Soc.* 2002; 124:11564–11565. [PubMed: 12296699] (b) Sharma GVM, Subash V, Narsimulu K, Sankar AR, Kunwar AC. *Angew Chem Int Ed.* 2006; 45:8207–8210. (c) Delsuc N, Hutin M, Campbell VE, Kauffmann B, Nitschke JR, Huc I. *Chemistry – A European Journal.* 2008; 14:7140–7143. (d) Lee BC, Chu TK, Dill KA, Zuckermann RN. *J Am Chem Soc.* 2008; 130:8847–8855. [PubMed: 18597438] (e) Petersson EJ, Schepartz A. *J Am Chem Soc.* 2008; 130:821–823. [PubMed: 18166055] (f) Price JL, Hadley EB, Steinkruger JD, Gellman SH. *Angew Chem Int Ed.* 2010; 49:368–371.
4. (a) Lu W, Qasim MA, Laskowski M, Kent SBH. *Biochemistry.* 1997; 36:673–679. [PubMed: 9020764] (b) Chapman E, Thorson JS, Schultz PG. *J Am Chem Soc.* 1997; 119:7151–7152. (c) Viles JH, Patel SU, Mitchell JBO, Moody CM, Justice DE, Uppenbrink J, Doyle PM, Harris CJ, Sadler PJ, Thornton JM. *J Mol Biol.* 1998; 279:973–986. [PubMed: 9642075] (d) Odaert B, Jean F, Melnyk O, Tartar A, Lippens G, Boutillon C, Buisine E. *Protein Sci.* 1999; 8:2773–2783. [PubMed: 10631995] (e) Arnold U, Hinderaker MP, Nilsson BL, Huck BR, Gellman SH, Raines RT. *J Am Chem Soc.* 2002; 124:8522–8523. [PubMed: 12121081] (f) Deechongkit S, Nguyen H, Powers ET, Dawson PE, Gruebele M, Kelly JW. *Nature.* 2004; 430:101–105. [PubMed: 15229605] (g) David R, Gunther R, Baumann L, Luhmann T, Seebach D, Hofmann HJ, Beck-Sickinge AG. *J Am Chem Soc.* 2008; 130:15311–15317. [PubMed: 18942784] (h) Lee BC, Zuckermann RN. *ACS Chem Biol.* 2011; 6:1367–1374. [PubMed: 21958072] (i) Valverde IE, Lecaille F, Lalmanach G, Aucagne V, Delmas AF. *Angew Chem Int Ed.* 2012; 51:718–722.
5. (a) Horne WS, Price JL, Gellman SH. *Proc Natl Acad Sci USA.* 2008; 105:9151–9156. [PubMed: 18587049] (b) Horne WS, Boersma MD, Windsor MA, Gellman SH. *Angew Chem Int Ed.* 2008; 47:2853–2856. (c) Horne WS, Johnson LM, Ketas TJ, Klasse PJ, Lu M, Moore JP, Gellman SH. *Proc Natl Acad Sci USA.* 2009; 106:14751–14756. [PubMed: 19706443]
6. (a) Lengyel GA, Frank RC, Horne WS. *J Am Chem Soc.* 2011; 133:4246–4249. [PubMed: 21370877] (b) Lengyel GA, Horne WS. *J Am Chem Soc.* 2012; 134:15906–15913. [PubMed: 22946450] (c) Lengyel GA, Eddinger GA, Horne WS. *Org Lett.* 2013; 15:944–947. [PubMed: 23390979]
7. Reinert ZE, Lengyel GA, Horne WS. *J Am Chem Soc.* 2013; 135:12528–12531. [PubMed: 23937097]
8. (a) Hagihara M, Anthony NJ, Stout TJ, Clardy J, Schreiber SL. *J Am Chem Soc.* 1992; 114:6568–6570. (b) Seebach D, Abele S, Gademann K, Jaun B. *Angew Chem Int Ed.* 1999; 38:1595–1597. (c) Karle IL, Gopi HN, Balaram P. *Proc Natl Acad Sci USA.* 2001; 98:3716–3719. [PubMed: 11259666] (d) Martinek TA, Toth GK, Vass E, Hollosi M, Fulop F. *Angew Chem Int Ed.* 2002; 41:1718–1721. (e) Langenhan JM, Guzei IA, Gellman SH. *Angew Chem Int Ed.* 2003; 42:2402–2405. (f) Bandyopadhyay A, Mali SM, Lunawat P, Raja KMP, Gopi HN. *Org Lett.* 2011; 13:4482–4485. [PubMed: 21815665]
9. (a) Searle MS, Ciani B. *Curr Opin Struct Biol.* 2004; 14:458–464. [PubMed: 15313241] (b) Nowick JS. *Acc Chem Res.* 2008; 41:1319–1330. [PubMed: 18798654]
10. Chatterjee J, Rechenmacher F, Kessler H. *Angew Chem Int Ed.* 2013; 52:254–269.
11. Spencer R, Chen KH, Manuel G, Nowick JS. *Eur J Org Chem.* 2013; 2013:3523–3528.
12. Fesinmeyer RM, Hudson FM, Andersen NH. *J Am Chem Soc.* 2004; 126:7238–7243. [PubMed: 15186161]
13. Searle MS, Griffiths-Jones SR, Maynard AJ. *J Mol Biol.* 1999; 292:1051–1069. [PubMed: 10512702]
14. (a) Fischer G. *Chem Soc Rev.* 2000; 29:119–127. (b) Dugave C, Demange L. *Chem Rev.* 2003; 103:2475–2532. [PubMed: 12848578]
15. Manavalan P, Momany FA. *Biopolymers.* 1980; 19:1943–1973. [PubMed: 6776998]

16. Hovmoller S, Zhou T, Ohlson T. *Acta Crystallogr Sect D Biol Crystallogr*. 2002; 58:768–776. [PubMed: 11976487]
17. (a) Gronenborn AM, Filpula DR, Essig NZ, Achari A, Whitlow M, Wingfield PT, Clore GM. *Science*. 1991; 253:657–661. [PubMed: 1871600] (b) Gallagher T, Alexander P, Bryan P, Gilliland GL. *Biochemistry*. 1994; 33:4721–4729. [PubMed: 8161530] (c) Frericks Schmidt HL, Sperling LJ, Gao YG, Wylie BJ, Boettcher JM, Wilson SR, Rienstra CM. *J Phys Chem B*. 2007; 111:14362–14369. [PubMed: 18052145]
18. (a) Fehrentz JA, Castro B. *Synthesis*. 1983:676–678. (b) Guichard G, Briand JP, Friede M. *Pept Res*. 1993; 6:121–124. [PubMed: 8318741]
19. (a) Debaene F, Mejias L, Harris JL, Winssinger N. *Tetrahedron*. 2004; 60:8677–8690. (b) Mali SM, Bandyopadhyay A, Jadhav SV, Kumar MG, Gopi HN. *Org Biomol Chem*. 2011; 9:6566–6574. [PubMed: 21826295]
20. Brunger AT. *Nat Protoc*. 2007; 2:2728–2733. [PubMed: 18007608]
21. Alexander P, Fahnestock S, Lee T, Orban J, Bryan P. *Biochemistry*. 1992; 31:3597–3603. [PubMed: 1567818]

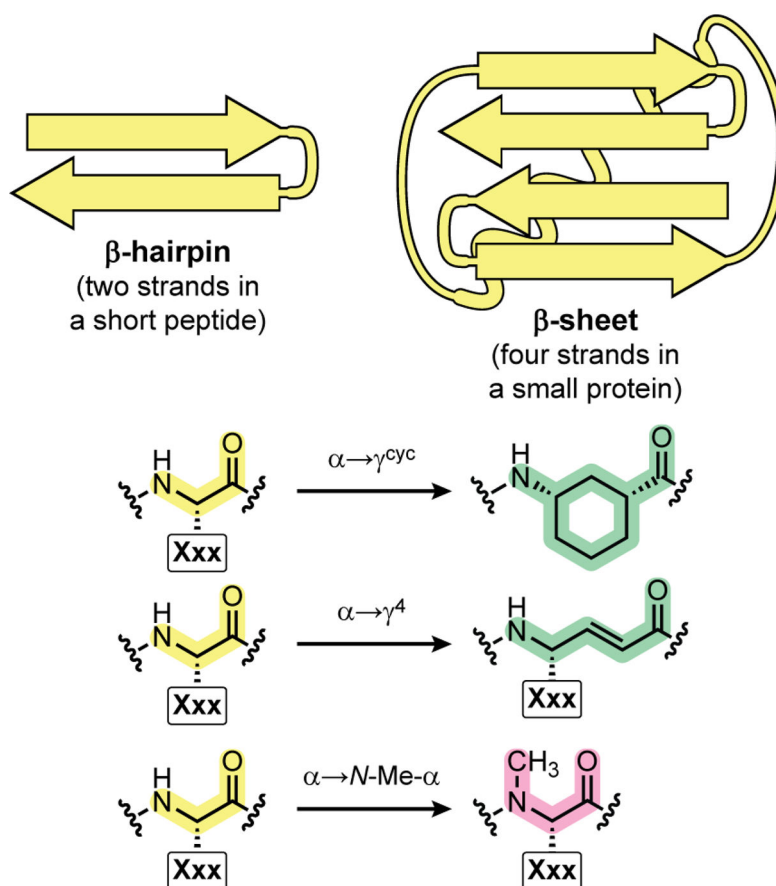


Fig. 1. Summary of strategies examined for peptide backbone modification in β -sheets. The impact of three different types of α -residue replacement on folding was evaluated in two different structural contexts, a β -hairpin peptide and a four-stranded β -sheet in a small protein.

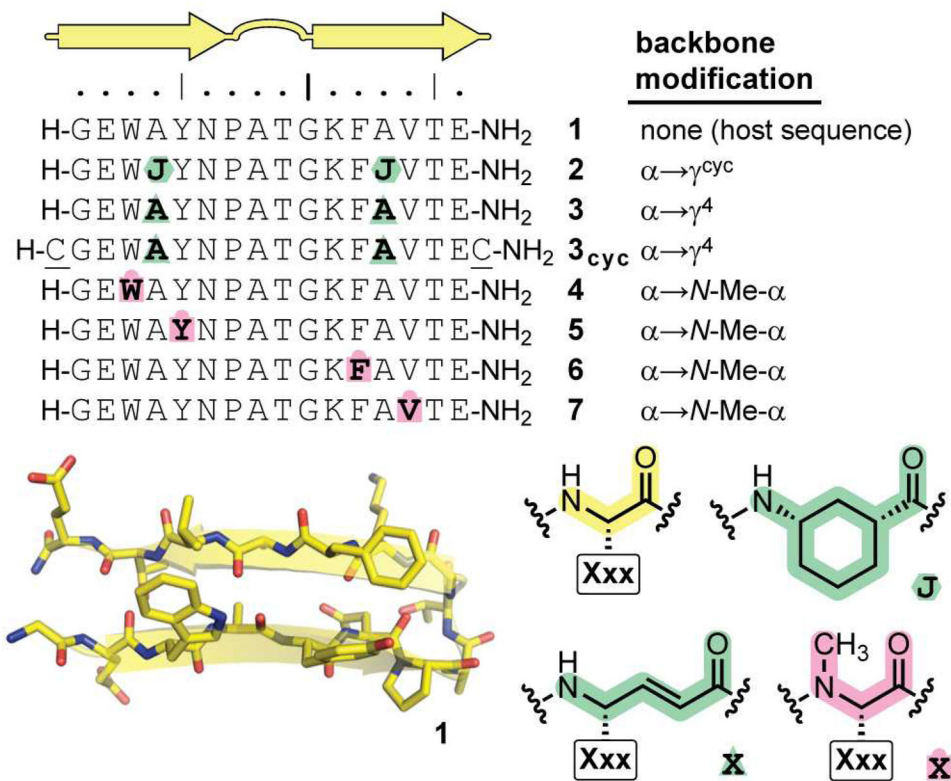


Fig. 2. Sequences of peptides **1–7**, key to α -residue replacements (Xxx indicates the side chain on the unnatural monomer is the same as the corresponding α -residue), and minimized average coordinates from the NMR solution structure of prototype peptide **1** in pH 6.3 phosphate buffer.

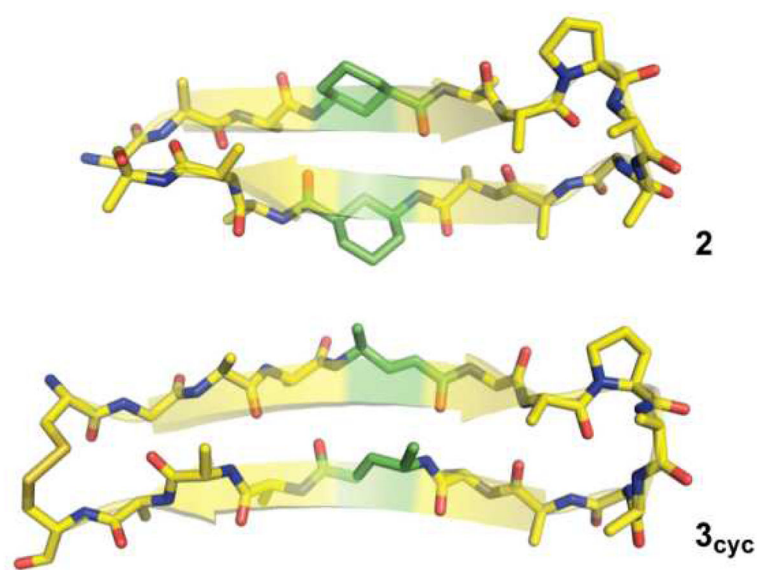
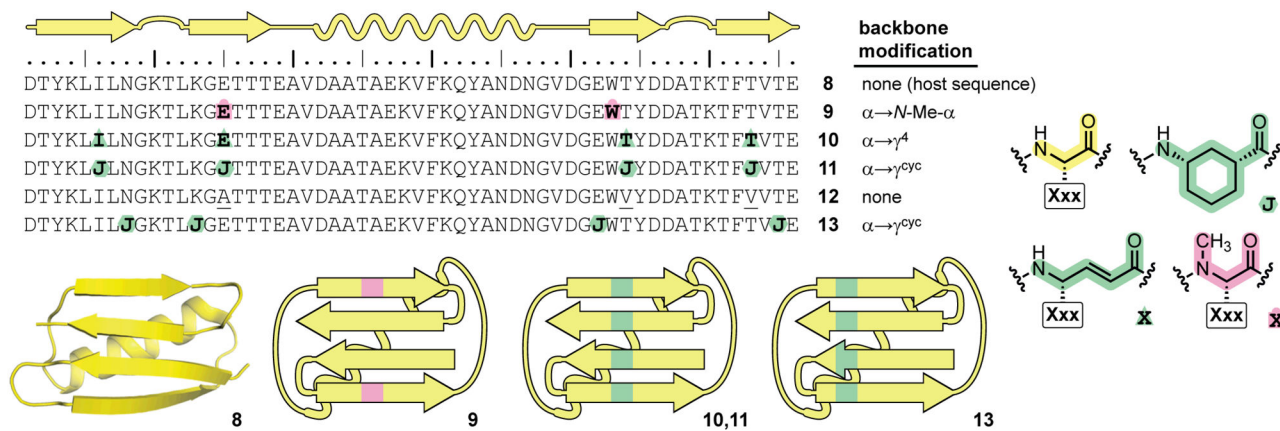


Fig. 3. Minimized average coordinates from NMR solution structures of $\alpha,\gamma^{\text{cyc}}$ -peptide **2** and α/γ^4 -peptide **3_{cyc}** in pH 6 phosphate buffer. Carbons are colored green for γ -residues and yellow for α -residues. Most side chains are omitted for clarity.



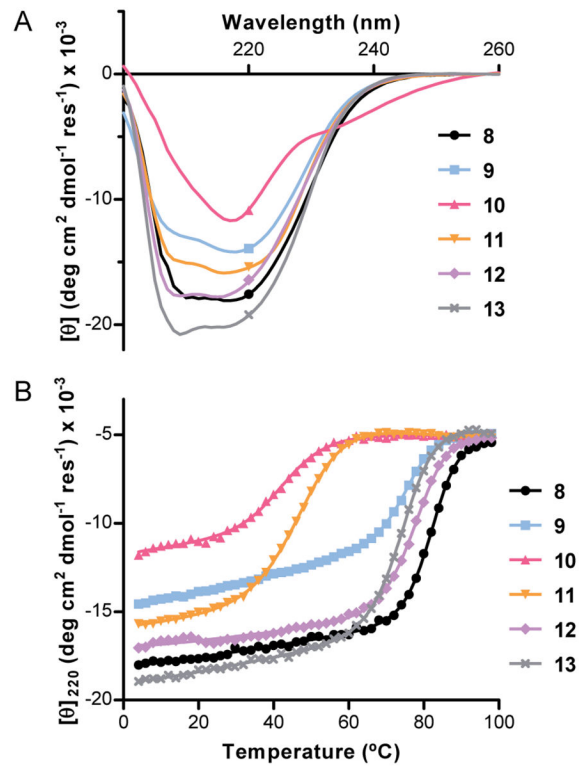


Fig. 5. Circular dichroism scans at 25 °C (A) and thermal melts monitored at 220 nm (B) for proteins 8–13. Experiments were carried out on 40 μ M concentration protein samples in 20 mM phosphate buffer, pH 7.

Table 1Folding thermodynamics of peptides 1–7 from NMR measurements^a

Peptide	δ Gly ₁₀ H _α /H _{α'} (ppm)	Fraction Folded (%)	G _{fold} (kcal mol ⁻¹)	G _{fold vs. 1} (kcal mol ⁻¹)
1	0.20	65	-0.3	
2	0.26	83	-0.9	-0.6
3	0.12	39	+0.2	+0.5
4		37 ^b	+0.3	+0.6
4 _{trans} (60%)	0.19	61	-0.3	+0.0
4 _{cis} (40%)	0.09			
5		19 ^b	+0.8	+1.1
5 _{trans} (76%)	0.09	30	+0.5	+0.8
5 _{cis} (24%)	0.00			
6		29 ^b	+0.5	+0.8
6 _{trans} (65%)	0.12	38	+0.3	+0.6
6 _{cis} (35%)	0.00			
7		55 ^b	-0.1	+0.2
7 _{trans} (87%)	0.20	63	-0.3	+0.0
7 _{cis} (13%)	0.12			

^aNMR carried out at 5 °C in pH 6.3 phosphate buffer. Assuming a 0.01 ppm uncertainty in measured Gly H_α/H_{α'} separation, error propagation estimates uncertainties of 5% for fraction folded and ~0.2 kcal mol⁻¹ for G_{fold} and G_{fold vs. 1}.

^bOverall folded population calculated as product of the fraction of peptide in the *trans* amide configuration and fraction folded for *trans* isomer.

Table 2Folding thermodynamics of proteins **8–13** from circular dichroism measurements^a

Protein	T_m (°C) ^a	G_{fold} vs. 8 (kcal mol ⁻¹)	substitutions vs. 8	G_{fold} per substitution (kcal mol ⁻¹)
8	82.1			
9	75.6	+1.1	2 $\alpha \rightarrow N\text{-Me-}\alpha$	0.6
10	43.5	+6.3	4 $\alpha \rightarrow \gamma^4$	1.6
11	46.7	+5.9	4 $\alpha \rightarrow \gamma^{\text{cyc}}$	1.5
12	78.0	+0.7	4 side chains	0.2
13	74.3	+1.3	4 $\alpha \rightarrow \gamma^{\text{cyc}}$	0.3

^aCD experiments carried out in pH 7 phosphate buffer

Author Manuscript

Author Manuscript

Author Manuscript

Author Manuscript